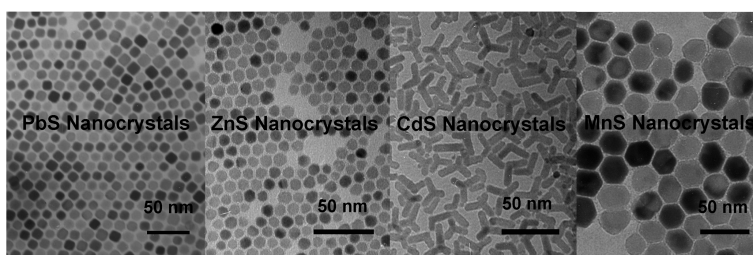


Generalized and Facile Synthesis of Semiconducting Metal Sulfide Nanocrystals

Jin Joo, Hyon Bin Na, Taekyung Yu, Jung Ho Yu, Young Woon Kim, Fanxin Wu, Jin Z. Zhang, and Taeghwan Hyeon

J. Am. Chem. Soc., **2003**, 125 (36), 11100-11105 • DOI: 10.1021/ja0357902 • Publication Date (Web): 13 August 2003

Downloaded from <http://pubs.acs.org> on March 29, 2009



More About This Article

Additional resources and features associated with this article are available within the HTML version:

- Supporting Information
- Links to the 56 articles that cite this article, as of the time of this article download
- Access to high resolution figures
- Links to articles and content related to this article
- Copyright permission to reproduce figures and/or text from this article

[View the Full Text HTML](#)

Generalized and Facile Synthesis of Semiconducting Metal Sulfide Nanocrystals

Jin Joo,[†] Hyon Bin Na,[†] Taekyung Yu,[†] Jung Ho Yu,[†] Young Woon Kim,[‡]
Fanxin Wu,[§] Jin Z. Zhang,[§] and Taeghwan Hyeon^{*†}

Contribution from the National Creative Research Initiative Center for Oxide Nanocrystalline Materials and School of Chemical Engineering and the School of Materials Science and Engineering, Seoul National University, Seoul 151-744, and Department of Chemistry, University of California, Santa Cruz, California 95064

Received April 25, 2003; E-mail: thyeon@plaza.snu.ac.kr

Abstract: We report on the synthesis of semiconductor nanocrystals of PbS, ZnS, CdS, and MnS through a facile and inexpensive synthetic process. Metal–oleylamine complexes, which were obtained from the reaction of metal chloride and oleylamine, were mixed with sulfur. The reaction mixture was heated under appropriate experimental conditions to produce metal sulfide nanocrystals. Uniform cube-shaped PbS nanocrystals with particle sizes of 6, 8, 9, and 13 nm were synthesized. The particle size was controlled by changing the relative amount of PbCl₂ and sulfur. Uniform 11 nm sized spherical ZnS nanocrystals were synthesized from the reaction of zinc chloride and sulfur, followed by one cycle of size-selective precipitation. CdS nanocrystals that consist of rods, bipods, and tripods were synthesized from a reaction mixture containing a 1:6 molar ratio of cadmium to sulfur. Spherical CdS nanocrystals (5.1 nm sized) were obtained from a reaction mixture with a cadmium to sulfur molar ratio of 2:1. MnS nanocrystals with various sizes and shapes were synthesized from the reaction of MnCl₂ and sulfur in oleylamine. Rod-shaped MnS nanocrystals with an average size of 20 nm (thickness) × 37 nm (length) were synthesized from a 1:1 molar ratio of MnCl₂ and sulfur at 240 °C. Novel bullet-shaped MnS nanocrystals with an average size of 17 nm (thickness) × 44 nm (length) were synthesized from the reaction of 4 mmol of MnCl₂ and 2 mmol of sulfur at 280 °C for 2 h. Shorter bullet-shaped MnS nanocrystals were synthesized from a 3:1 molar ratio of MnCl₂ and sulfur. Hexagon-shaped MnS nanocrystals were also obtained. All of the synthesized nanocrystals were highly crystalline.

Introduction

Colloidal nanocrystals have attracted broad attention from researchers in various disciplines.¹ These nanocrystals exhibit size-dependent characteristics, and they often exhibit novel electronic, magnetic, optical, chemical, and mechanical properties that cannot be obtained in their bulk counterparts.² Among the various nanocrystals, colloidal semiconductor nanocrystals, representatively metal chalcogenide nanocrystals, have been the most studied due to their quantum confinement effects and size-dependent photoemission characteristics.³ These semiconductor nanocrystals have been applied to many different technological

areas including biological labeling and diagnostics, light-emitting diodes, electroluminescent devices, photovoltaic devices, lasers, and single-electron transistors.⁴ Semiconductor nanocrystals having variable sizes and different shapes have been synthesized by various solution-phase synthetic schemes including the most popular organometallic synthetic procedure employing the high-temperature thermolysis of precursors.⁵ Through these synthetic procedures, nanocrystals are produced with typical particle size distributions of $\sim\sigma$ 10%. Further size-selection processes allow the particle size distribution to be reduced to below σ 5% to obtain monodisperse nanocrystals. CdSe nanocrystals have been the most intensively studied, while relatively little work has been done on semiconductor sulfide nanocrystals. Sulfide nanocrystals, including CdS nanocrystals, were synthesized from the reaction of alkaline aqueous metal salt with H₂S in the presence of a suitable stabilizing agent.⁶ Recently, several groups reported

[†] National Creative Research Initiative Center for Oxide Nanocrystalline Materials and School of Chemical Engineering, Seoul National University.

[‡] School of Materials Science and Engineering, Seoul National University.

[§] University of California, Santa Cruz.

- (1) (a) Klabunde, K. J. *Nanoscale Materials in Chemistry*; Wiley-Interscience: New York, 2001. (b) Fendler, J. H. *Nanoparticles and Nanostructured Films*; Wiley-VCH: Weinheim, Germany, 1998. (c) Weller, H. *Angew. Chem., Int. Ed. Engl.* **1993**, *32*, 41. (d) Rogach, A. L.; Talapin, D. V.; Shevchenko, E. V.; Kornowski, A.; Haase, M.; Weller, H. *Adv. Funct. Mater.* **2002**, *12*, 653.
- (2) (a) Sun, S.; Murray, C. B.; Weller, D.; Folks, L.; Moser, A. *Science* **2000**, *287*, 1989. (b) Hyeon, T. *Chem. Commun.* **2003**, 927. (c) Nirmal, M.; Brus, L. E. *Acc. Chem. Res.* **1999**, *32*, 407. (d) Jacobs, K.; Zaziski, D.; Scher, E. C.; Herhold, A. B.; Alivisatos, A. P. *Science* **2001**, *293*, 1803. (e) Michler, P.; Imamoglu, A.; Mason, M. D.; Carson, P. J.; Strouse, G. F.; Buratto, S. K. *Nature* **2000**, *406*, 968. (f) Kim, S.-W.; Son, S. U.; Lee, S. S.; Hyeon, T.; Chung, Y. K. *Chem. Commun.* **2001**, 2212.

- (3) (a) Alivisatos, A. P. *Science* **1996**, *271*, 933. (b) Murray, C. B.; Kagan, C. R.; Bawendi, M. G. *Annu. Rev. Mater. Sci.* **2000**, *30*, 545. (c) Bawendi, M. G.; Steigerwald, M. L.; Brus, L. E. *Annu. Rev. Phys. Chem.* **1990**, *41*, 477.

- (4) (a) Hu, J.; Li, L.-S.; Yang, W.; Manna, L.; Wang, L.-W.; Alivisatos, A. P. *Science* **2001**, *292*, 2060. (b) Sundar, V. C.; Eisler, H.-J.; Bawendi, M. G. *Adv. Mater.* **2002**, *14*, 739. (c) Tessler, N.; Medvedev, V.; Kazes, M.; Kan, S.; Banin, U. *Science* **2002**, *295*, 1506. (d) Brunchez, M. P.; Moronne, M.; Gin, P.; Weiss, S.; Alivisatos, A. P. *Science* **1998**, *281*, 2013. (e) Chan, W. C. W.; Nie, S. *Science* **1998**, *281*, 2016.

the synthesis of sulfide nanocrystals from the thermolysis of single-source precursors.⁷ Peng and co-workers⁸ reported the synthesis of cadmium chalcogenide nanocrystals through green chemical approaches employing CdO or Cd-hexylphosphonic acid as precursors and noncoordinating solvents. As part of our continuing effort to synthesize monodisperse nanocrystals, here we report on the synthesis of semiconductor sulfide nanocrystals of lead, manganese, zinc, and cadmium through a facile and inexpensive synthetic process.

Experimental Section

Synthesis of PbS Nanocrystals. PbCl₂ (1 mmol, 0.28 g) was added to 5 mL of oleylamine at room temperature and the resulting solution was heated to 90 °C under vacuum, forming a homogeneous and clear solution. Elemental sulfur (0.83 mmol, 27 mg) was dissolved in 2.5 mL of oleylamine, and the resulting sulfur solution was injected into the Pb-oleylamine complex solution at 90 °C. The resulting mixture was heated to 220 °C and aged at that temperature for 1 h, resulting in a black colloidal solution. Ethanol (100 mL) was added in order to cause the PbS nanocrystals to be precipitated. The precipitate was retrieved by centrifugation, producing deep blue colored PbS nanocrystals. The nanocrystals are dispersible in many organic solvents, such as toluene, hexane, and octane.

Synthesis of ZnS Nanocrystals. ZnS nanocrystals were synthesized from the reaction of ZnCl₂ and sulfur in oleylamine in the presence of trioctylphosphine oxide (TOPO). Zinc-oleylamine solution was prepared by heating 10 mL of oleylamine and 2.3 g of TOPO containing 2 mmol of ZnCl₂ at 170 °C for 1 h. Sulfur (6 mmol) dissolved in 2.5 mL of oleylamine was injected into zinc-oleylamine solution at room temperature. This mixture was heated to 320 °C and aged for 1 h at the same temperature. ZnS nanocrystals were separated by adding excess ethanol followed by centrifugation. Collected ZnS nanocrystals were dispersed in hexane.

Synthesis of CdS Nanocrystals. From the reaction of CdCl₂ and sulfur in oleylamine, we were able to synthesize CdS nanocrystals with various sizes and shapes. Rod-shaped CdS nanocrystals were synthesized from a reaction mixture with a cadmium to sulfur molar ratio of 1:6. More specifically, 1 mmol of CdCl₂ in 10 mL of oleylamine was heated at 90 °C to generate Cd-oleylamine complexes. Sulfur (6 mmol) in 5 mL of oleylamine was injected into the Cd-oleylamine complexes at 90 °C. The resulting mixture was heated to 140 °C and aged at that temperature for 20 h. Spherical-shaped CdS nanocrystals were synthesized from a reaction mixture with a cadmium to sulfur molar ratio of 2:1. Sulfur (0.75 mmol) in 5 mL of oleylamine was injected into a oleylamine solution containing 1.5 mmol of cadmium-oleylamine

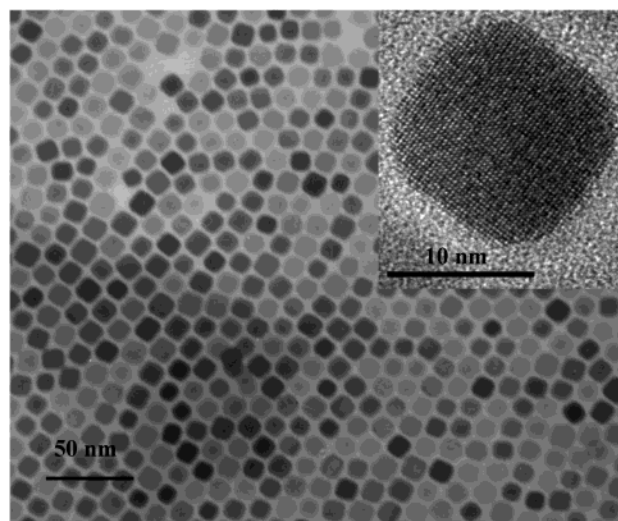


Figure 1. Low-magnification TEM image of 13 nm PbS nanocrystals; inset is HRTEM image of a single 13 nm PbS nanocrystal.

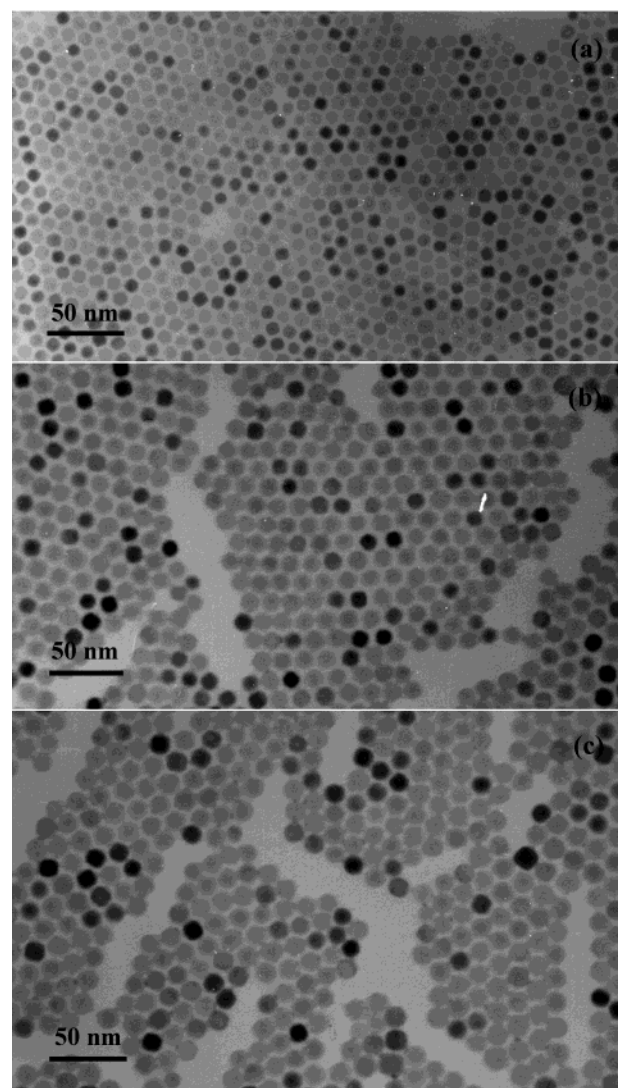


Figure 2. TEM images of (a, top) 6 nm, (b, middle) 8 nm, and (c, bottom) 9 nm sized PbS nanocrystals.

complex at 160 °C. The resulting mixture was aged for 6 h at that temperature. The resulting CdS nanocrystals were retrieved by adding ethanol followed by centrifugation.

- (5) (a) Murray, C. B.; Norris, D. J.; Bawendi, M. G. *J. Am. Chem. Soc.* **1993**, *115*, 8706. (b) Peng, X.; Wickham, J.; Alivisatos, A. P. *J. Am. Chem. Soc.* **1998**, *120*, 5343. (c) Peng, Z. A.; Peng, X. *J. Am. Chem. Soc.* **2002**, *124*, 3343. (d) Talapin, D. V.; Rogach, A. L.; Shevchenko, E. V.; Kornowski, A.; Haase, M.; Weller, H. *J. Am. Chem. Soc.* **2002**, *124*, 5782. (e) DeGroot, M. W.; Taylor, N. J.; Corrigan, J. F. *J. Am. Chem. Soc.* **2003**, *125*, 864. (f) Shim, M.; Guyot-Sionnest, P. *Nature* **2000**, *407*, 981. (g) Peng, X. *Adv. Mater.* **2003**, *15*, 459. (h) Talapin, D. V.; Rogach, A. L.; Kornowski, A.; Haase, M.; Weller, H. *Nano Lett.* **2001**, *1*, 207. (i) Talapin, D. V.; Rogach, A. L.; Mekis, I.; Haubold, S.; Kornowski, A.; Haase, M.; Weller, H. *Colloids Surf. A* **2002**, *202*, 145. (j) Qu, L.; Peng, Z. A.; Peng, G. *Nano Lett.* **2001**, *1*, 333. (k) Kan, S. H.; Felner, I.; Banin, U. *Isr. J. Chem.* **2001**, *41*, 55. (l) Lazell, M.; O'Brien, P. *J. Mater. Chem.* **1999**, *9*, 1381. (m) Wang, W.; Geng, Y.; Yan, P.; Liu, F.; Xie, Y.; Qian, Y. *J. Am. Chem. Soc.* **1999**, *121*, 4062. (n) Redl, F. X.; Cho, K. S.; Murray, C. B.; O'Brien, S. *Nature* **2003**, *423*, 968.
- (6) Steigerwald, M. L.; Alivisatos, A. P.; Gibson, J. M.; Harris, T. D.; Kortan, R.; Muller, A. J.; Thayer, A. M.; Duncan, T. M.; Douglass, D. C.; Brus, L. E. *J. Am. Chem. Soc.* **1988**, *110*, 3046.
- (7) (a) Lee, S.-M.; Jun, Y.-W.; Cho, S.-N.; Cheon, J. *J. Am. Chem. Soc.* **2002**, *124*, 11244. (b) Jun, Y.-W.; Jung, Y.-Y.; Cheon, J. *J. Am. Chem. Soc.* **2002**, *124*, 615. (c) Cumberland, S. L.; Hanif, K. M.; Javier, A.; Khitrov, G. A.; Strouse, G. F.; Woessner, S. M.; Yun, C. S. *Chem. Mater.* **2002**, *14*, 1576. (d) Pradhan, N.; Efrima, S. *J. Am. Chem. Soc.* **2003**, *125*, 2050.
- (8) (a) Peng, X. *Chem. Eur. J.* **2002**, *8*, 335. (b) Yu, M. W.; Peng, X. G. *Angew. Chem., Int. Ed.* **2002**, *41*, 2368. (c) Peng, Z. A.; Peng, X. G. *J. Am. Chem. Soc.* **2001**, *123*, 183.

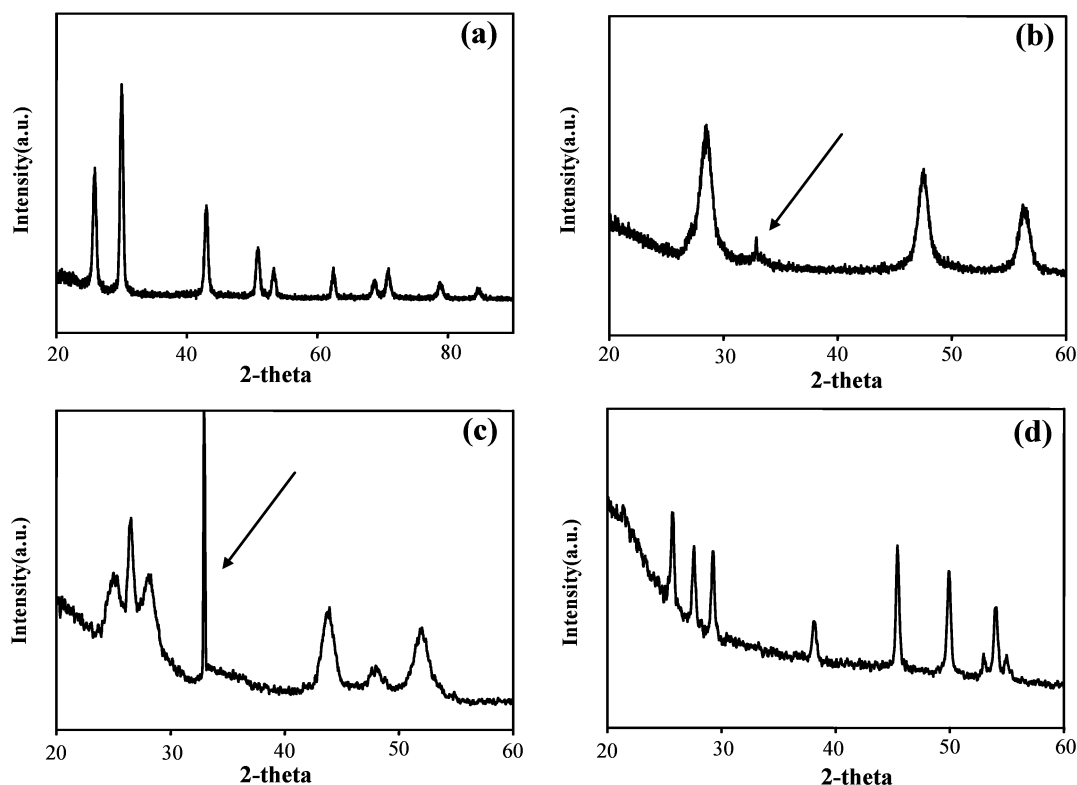


Figure 3. X-ray diffraction patterns of (a) PbS nanocrystals, cubic ($Fm\bar{3}m$) structure; (b) ZnS nanocrystals, zinc blende structure; (c) CdS nanocrystals, wurtzite structure; and (d) hexagon-shaped MnS nanocrystals, wurtzite structure. The peaks indicated by arrows are Si substrate peak.

Synthesis of MnS Nanocrystals. Rod-shaped MnS nanocrystals were synthesized as follows. Homogeneous Mn–oleylamine complexes were prepared by reacting 2 mmol of $MnCl_2$ and 10 mL of oleylamine at 120 °C. Elemental sulfur (2 mmol) was dissolved in 5 mL of oleylamine at room temperature. The sulfur solution was injected into the Mn–oleylamine complex and the resulting solution was aged at 240 °C for 2 h. MnS nanocrystals were separated by adding excess ethanol followed by centrifugation.

Bullet-shaped MnS nanocrystals were synthesized by the following synthetic procedure. Manganese–oleylamine complex was prepared by reacting 4 mmol of $MnCl_2$ and 10 mL of oleylamine at 120 °C. Sulfur (2 mmol) dissolved in 5 mL of oleylamine was added into the manganese–oleylamine complex at 60 °C and the resulting mixture was aged for 2 h at 280 °C. Hexagon-shaped MnS nanocrystals were synthesized from aging of the reaction mixture containing 6 mmol of $MnCl_2$ and 2 mmol of sulfur at 280 °C for 6 h.

Characterization of Materials. Nanocrystals were characterized by low- and high-resolution transmission electron microscopy (TEM), electron diffraction, and X-ray diffraction. Low-resolution transmission electron micrographs were obtained on a Jeol EM-2010 microscope. High-resolution transmission electron micrographs were taken on a Jeol JEM-3000F microscope. X-ray diffraction pattern was obtained with a Rigaku D/Max-3C diffractometer equipped with a rotating anode and a Cu KR radiation source ($\lambda = 0.15418$ nm).

The optical properties of the CdS and ZnS nanocrystals have been characterized by electronic absorption and fluorescence spectroscopy. The electronic absorption and fluorescence spectra have been obtained on a Hewlett-Packard 8425A diode-array UV–visible spectrometer and a Perkin-Elmer fluorometer (LS50B), respectively. Fluorescence quantum yield has been calculated by integrating the fluorescence band of CdS nanocrystals in cyclohexane or ZnS in octane and comparing to that of perylene in ethanol, assuming the fluorescence quantum yield of perylene in ethanol excited at the same wavelength is 99%.⁹

(9) Melhuish, W. H. *J. Phys. Chem.* **1961**, *65*, 229.

Results and Discussion

The current synthetic procedure is a modified version of the method used by our group for the synthesis of monodisperse nanocrystals of metal oxides, which employs the formation of a metal–surfactant complex followed by aging at high temperature.¹⁰ Metal chlorides and elemental sulfur were used as reactants. Under optimized reaction conditions, multiple grams of nanocrystals can be produced without a size-selection process. Metal chloride was dissolved in oleylamine to form a metal–oleylamine complex. Into the resulting solution, elemental sulfur dissolved in oleylamine was injected at an appropriate temperature. The mixture solution was slowly heated to generate metal sulfide nanocrystals.

Synthesis of PbS Nanocrystals. PbS is a semiconductor with a band gap energy of 0.41 eV and could find applications such as near-IR communication. PbS nanocrystals offer unique access to the regime of extreme quantum confinement since the electron, hole, and exciton all have relatively large Bohr radii of 20 nm.¹¹ Here we were able to synthesize PbS nanocrystals with particle sizes smaller than the Bohr radius. The transmission electron microscopic (TEM) image of the PbS nanocrystals shown in Figure 1 revealed uniform 13 nm sized nanocrystals. The particle shape is nearly cubic, and the high-resolution transmission electron microscopic (HRTEM) image of a single nanocrystal exhibited a cross lattice pattern, demonstrating

- (10) (a) Hyeon, T.; Lee, S. S.; Park, J.; Chung, Y.; Na, H. B. *J. Am. Chem. Soc.* **2001**, *123*, 12798. (b) Hyeon, T.; Chung, Y.; Park, J.; Lee, S. S.; Kim, Y.-W.; Park, B. H. *J. Phys. Chem. B* **2002**, *106*, 6831. (c) Joo, J.; Yu, T.; Kim, Y.-W.; Park, H. M.; Wu, F.; Zhang, J. Z.; Hyeon, T. *J. Am. Chem. Soc.* **2003**, *125*, 6553.
- (11) (a) Frank, W. W. *Acc. Chem. Res.* **2000**, *33*, 773. (b) Zhou, Y.; Itoh, H.; Uemura, T.; Naka, K.; Chujo, Y. *Langmuir* **2002**, *18*, 5287. (c) Wang, S.; Yang, S. *Langmuir* **2000**, *16*, 389. (d) Chen, S.; Truax, L. A.; Sommers, J. M. *Chem. Mater.* **2000**, *12*, 3864.

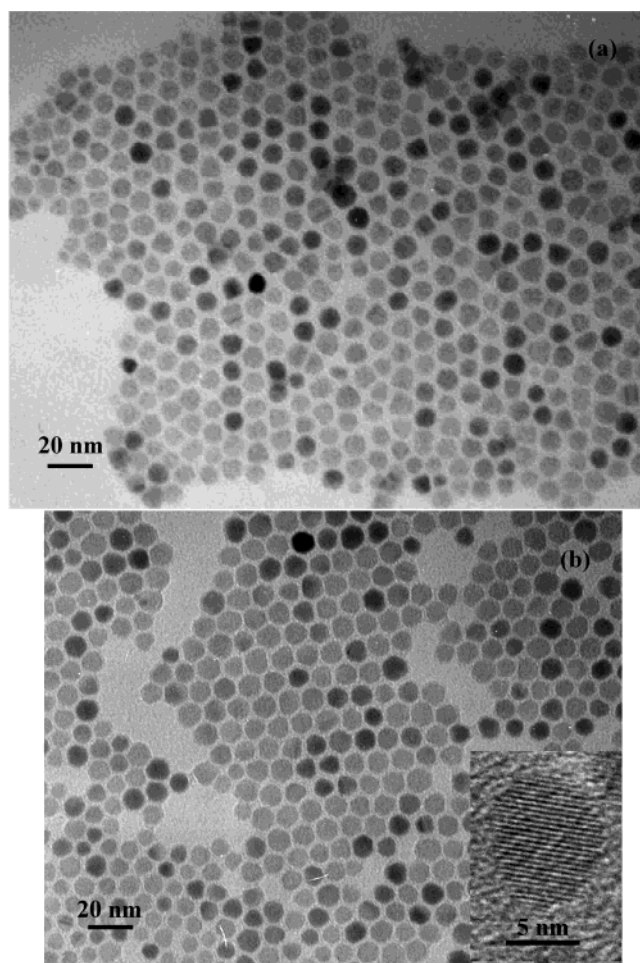


Figure 4. TEM images of ZnS nanocrystals: (a) before size-selection process; (b) after size-selection process. Inset is HRTEM image of a single ZnS nanocrystal.

the highly crystalline nature of the nanocrystals (Figure 1). Powder X-ray diffraction (XRD) of the nanocrystals, shown in Figure 3a, revealed the cubic rock-salt structure of PbS. Crystal size of PbS nanocrystals calculated from the Scherrer formula was 13.7 nm. The particle size of PbS nanocrystals can be controlled by changing the relative amount of PbCl_2 and sulfur. For example, using a fixed 1 mmol of PbCl_2 , and 0.33, 0.50, and 0.67 mmol of sulfur, we synthesized PbS nanocrystals with sizes of 6, 8, and 9 nm, respectively. Figure 2 shows TEM images of these PbS nanocrystals. Smaller-sized nanocrystals are nearly spherical, whereas larger nanocrystals exhibited cubic shape. This sphere-to-cube transition of PbS nanocrystals was reported earlier by other researchers.^{7a}

Synthesis and Optical Properties of ZnS Nanocrystals. As prepared, ZnS nanocrystals have a size distribution ranging from 7 to 11 nm (Figure 4a). Crystal size of ZnS nanocrystals before the size-selection process, calculated from the Scherrer formula, was 8.2 nm. After one cycle of a size-selective process involving the addition of an appropriate amount of ethanol into the hexane solution of nanocrystals, we obtained uniform spherical-shaped ZnS nanocrystals with a particle size of 11 nm (Figure 4b). A low-magnification TEM image of ZnS nanocrystals (Figure 4b) showed uniform nanoparticles with particle size of 11 nm. A high-resolution TEM (HRTEM) image of a single nanocrystal revealed highly crystalline nature of ZnS nanocrystals. The XRD pattern of ZnS nanocrystal, shown in Figure 3b, revealed a zinc

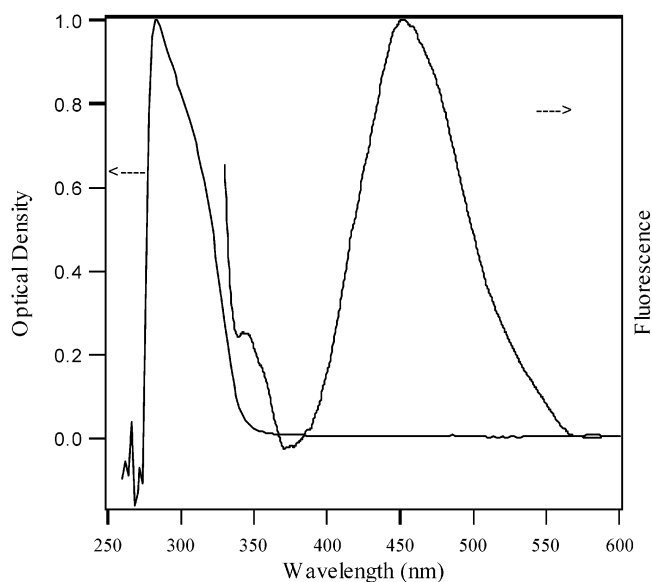


Figure 5. Representative electronic absorption spectrum (left) and static fluorescence spectrum (right) of ZnS nanoparticles in octane. For the fluorescence spectrum, the sample was excited at 320 nm. Fluorescence quantum yield was calculated to be 1.0%.

blende structure. Trioctylphosphine oxide (TOPO) was added to the reaction mixture along with oleylamine for the effective dispersion of nanocrystals. The size uniformity of the current synthesized ZnS nanocrystals is the best among the reported data.

Figure 5 shows the representative electronic absorption and fluorescence spectra of ZnS nanoparticles in octane. The absorption spectrum shows an excitonic peak at around 310 nm. The fluorescence spectrum shows peaks at 342 and 450 nm. The solvent fluorescence signal at 370 nm has been subtracted. The peak at 450 nm is attributed to the trap states emission of ZnS nanocrystals due to the broad feature and substantial red shift of the band. The peak at 342 nm has been assigned to band edge emission. The fluorescence quantum yield of ZnS nanocrystals has been calculated to 1.0% for excitation at 320 nm. [Note: Perylene shows strong absorption peaks in the range from 380 to 450 nm (data not shown) and very weak absorption at 320 nm. To reduce the error in measuring the OD of low-concentration perylene/ethanol solution at 320 nm, the OD at 320 nm has been calculated from the OD of low-concentration perylene/ethanol at 390 nm and the ratio of the OD at 320 and 390 nm of high-concentration perylene/ethanol.]

Synthesis and Optical Properties of CdS Nanocrystals. In the previous work by Cheon and co-workers,^{7b,12a,d} they synthesized sulfide nanocrystals with various shapes by controlling the reaction temperature. However, in the current synthesis, we were able to control the shapes of CdS nanocrystals by varying the molar ratio of cadmium chloride and sulfur at low reaction temperature. When a 1:6 molar ratio of cadmium to sulfur was used in the synthesis, CdS nanocrystals that consist of rods, bipods, and tripods were obtained. A TEM image of the CdS nanocrystals, shown in Figure 6a, revealed that these

(12) (a) Lee, S.-M.; Cho, S.-N.; Cheon, J. *Adv. Mater.* **2003**, *15*, 441. (b) Peng, X.; Manna, L.; Yang, W.; Wickham, J.; Scher, E.; Kadavanich, A.; Alivisatos, A. P. *Nature* **2000**, *404*, 59. (c) Manna, L.; Scher, E. C.; Alivisatos, A. P. *J. Am. Chem. Soc.* **2000**, *122*, 12700. (d) Jun, Y.-W.; Lee, S.-M.; Kang, N.-J.; Cheon, J. *J. Am. Chem. Soc.* **2001**, *123*, 5150. (e) Peng, Z. A.; Peng, X. G. *J. Am. Chem. Soc.* **2001**, *123*, 1389.

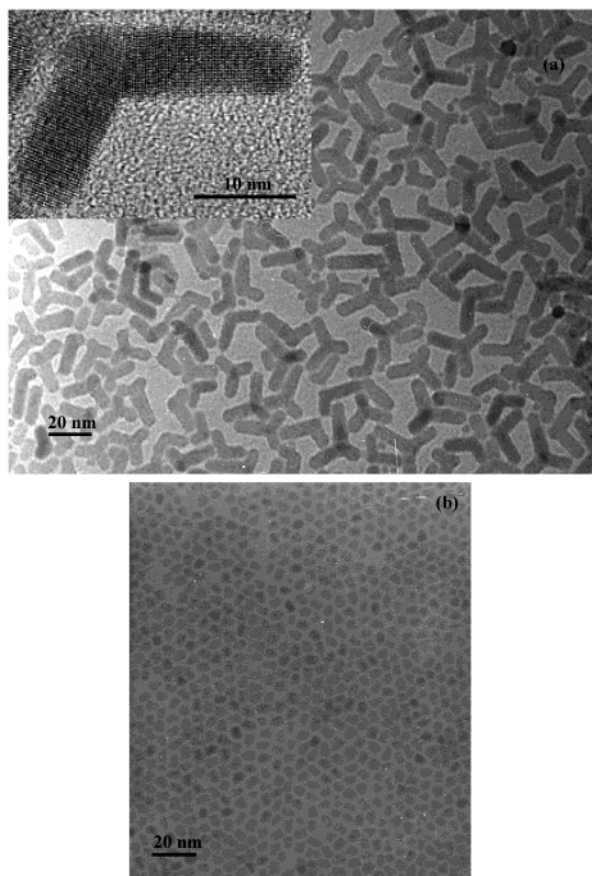


Figure 6. TEM images of CdS nanocrystals. (a) Mixture of rods, bipods, and tripods with an average size of 5.4 nm (thickness) \times 20 nm (length); inset is a HRTEM image of a single CdS bipod-shaped nanocrystal. (b) Spherical nanoparticles with an average diameter of 5.1 nm.

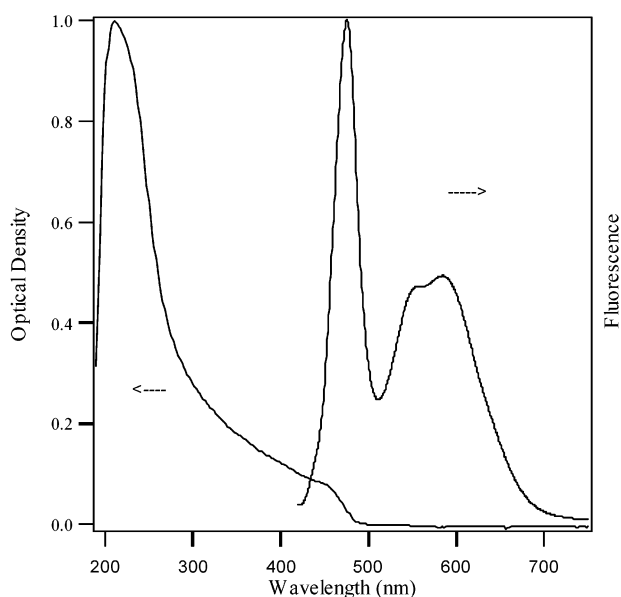


Figure 7. Representative electronic absorption spectrum (left) and static fluorescence spectrum (right) of 5.1 nm spherical CdS nanocrystals in cyclohexane. For the fluorescence spectrum, the sample was excited at 390 nm. Fluorescence quantum yield was calculated to be 0.43%.

rod-shaped nanocrystals have an average thickness of 5.4 nm and an average length of 20 nm.¹² The XRD pattern of the nanocrystals revealed a wurtzite crystal structure (Figure 3c).

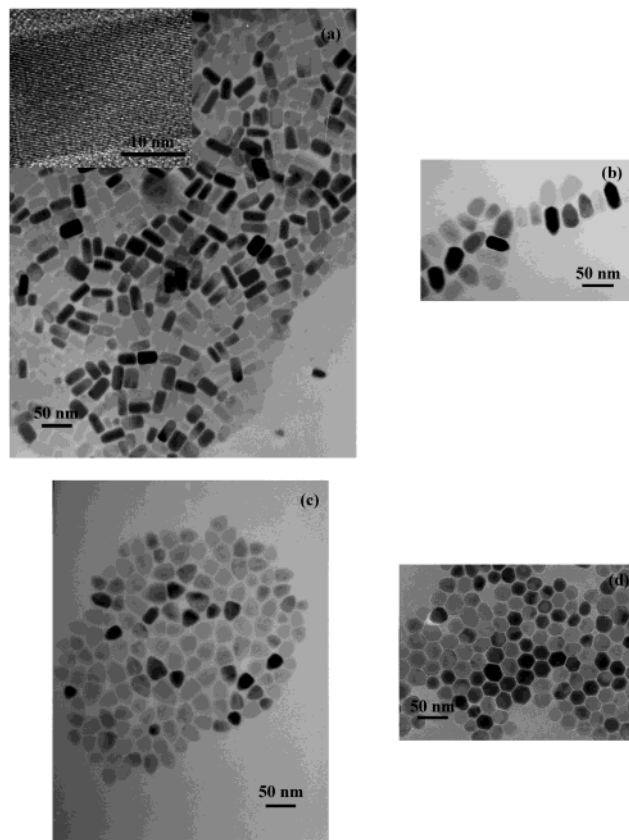


Figure 8. TEM images of MnS nanocrystals. (a) MnS nanorods. Inset is a HRTEM image of a single MnS nanorod. (b) Long bullet-shaped MnS nanocrystals. (c) Short bullet-shaped MnS nanocrystals. (d) Hexagon-shaped MnS nanocrystals.

Figure 6b shows the TEM image of 5.1 nm sized spherical CdS nanocrystals synthesized from a reaction mixture with a cadmium to sulfur molar ratio of 2:1. Figure 7 shows the representative electronic absorption and fluorescence spectra of spherical 5.1 nm sized CdS nanocrystals in cyclohexane. The absorption spectrum features an excitonic peak around 472 nm (2.63 eV), indicating a particle size of about 4.5 nm in diameter.¹³ Fluorescence spectra of the spherical CdS nanocrystals were measured with several excitation wavelengths from 350 to 420 nm. While the fluorescence intensity changes somewhat with excitation wavelength, the fluorescence peak position and band shape remain the same. This indicates that the fluorescence involves the same initial and final states even as the excitation wavelength was varied between 350 and 420 nm, suggesting fast relaxation from the final state reached by photoexcitation to the states from which the fluorescence originates. The fluorescence spectrum of the spherical CdS nanocrystals shows a band edge emission at 476 nm and a broad trap state emission centered around 584 nm. The broad feature of the trap state emission band indicates that there is a large number of trap states. This is consistent with the relatively low fluorescence quantum yield of 0.43% at 390 nm. The double-peaked trap state emission band indicates two sets of trap states. Both spherical ZnS and CdS nanocrystals exhibited moderate photoluminescence yields. Strongly luminescent CdS and ZnS nanoparticles can have yields over 10%, with predominantly band edge emission and little trap state emission. Weakly

(13) Wang, Y.; Herron, N. *J. Phys. Chem.* **1991**, *95*, 525.

luminescent CdS and ZnS nanocrystals typically have yields of <0.1%, with predominantly trap state emission and little band edge emission. Moderately luminescent CdS and ZnS nanocrystals have quantum yields in the range of 0.3%–3% with comparable band edge and trap state emission. The nanocrystals samples studied here fall into this moderately luminescent range.

Synthesis of MnS Nanocrystals. MnS nanocrystals with various sizes and shapes were synthesized from the reaction of MnCl_2 and sulfur in oleylamine. TEM image of MnS nanocrystals synthesized from a 1:1 molar ratio of MnCl_2 and sulfur at 240 °C (Figure 8a) showed rod-shaped MnS nanocrystals with an average size of 20 nm (thickness) \times 37 nm (length). The HRTEM image of a single MnS nanorod (inset of Figure 8a) showed (001) lattice plane, confirming the highly crystalline nature of the nanocrystal. We were able to control the size of the nanorods by changing the reaction temperature. As the reaction temperature was increased, the length of MnS nanorods was increased up to 60 nm.

Figure 8b shows the TEM image of novel bullet-shaped MnS nanocrystals with an average size of 17 nm (thickness) \times 44 nm (length) that were synthesized from the reaction of 4 mmol of MnCl_2 and 2 mmol of sulfur at 280 °C for 2 h. Shorter bullet-shaped MnS nanocrystals were synthesized from a 3:1 molar ratio of MnCl_2 and sulfur (Figure 8c). The TEM image of novel

hexagon-shaped MnS nanocrystals is shown in Figure 8d. The XRD patterns of these MnS nanocrystals revealed a wurtzite crystal structure (γ -MnS) (Figure 3d).

Conclusion

We synthesized semiconducting metal sulfide nanocrystals of PbS, ZnS, CdS, and MnS with various sizes and shapes from the thermal reaction of metal chloride and sulfur in oleylamine. The synthetic procedures developed in the present study offer several very important advantageous features for the synthesis of sulfide nanocrystals. First, the synthetic process is environmentally friendly and inexpensive, which employs inexpensive and nontoxic reagents such as metal chlorides and sulfur. Second, the synthetic method is a generalized process that can be applied to synthesize different kinds of sulfide nanocrystals having various particle sizes and shapes. Third, the process allows uniform-sized sulfide nanocrystals to be obtained without a further size-selection process and the indications are that scale-up can be achieved relatively easily.

Acknowledgment. The work was supported by the National Creative Research Initiative Program of the Korean Ministry of Science and Technology.

JA0357902